ly stimulate the haltere control muscles without also directly activating afferents within the adjacent haltere nerve.

The haltere efferent control pathway is based on a neural architecture that may be common among insects and provides a parsimonious explanation for the evolution of halteres from aerodynamically functional hind wings. In locusts, hind wing mechanoreceptors make strong connections with fore wing motoneurons and function to maintain a correct phase relation between the metathoracic and mesothoracic wing pairs (*32*). Although the hind wings of flies have lost all aerodynamic function, they have retained and elaborated mechanoreceptors capable of entraining motoneurons of the fore wing. Wings, like halteres, are susceptible to Coriolis forces. However, without using a sophisticated multiplexing strategy, it would be difficult for the nervous system to distinguish between aerodynamic forces and Coriolis force acting on wings. The reduction of the halteres' aerodynamic role may have resulted from disruptive selection acting to specialize the fore wing as an aerodynamic organ and the hind wing as a Coriolis force-sensitive equilibrium organ. Although the haltere efferent system provides a sophisticated means of integrating visual and mechanosensory information, the underlying circuitry probably arose from a general pattern of segmentally repeated sensory-motor reflexes.

REFERENCES AND NOTES

1. T. S. Collett and M. F. Land, *J. Comp. Physiol. A* **99**, 1 (1975).
2. H. Wagner, *Philos. Trans. R. Soc. London Ser. B* **312**, 553 (1986).
3. H. Autrum, *Exp. Cell Res. Suppl.* **5**, 426 (1958).
4. F.-O. Lehmann and M. H. Dickinson, *J. Exp. Biol.* **201**, 385 (1998).
5. G. Fraenkel and J. W. S. Pringle, *Nature* **141**, 919 (1938); G. Schneider, *Z. Vgl. Physiol.* **35**, 416 (1953).
6. H. Pflugstaedt, *Z. Wiss. Zool.* **100**, 1 (1912).
7. W. Gnatzy, U. Grünert, M. Bender, *Zoomorphology* **106**, 312 (1987); W. P. Chan and M. H. Dickinson, *J. Comp. Neurol.* **369**, 405 (1996).
8. R. Faust, *Zool. Jahrb. Abt. Allg. Zool. Physiol. Tiere* **63**, 325 (1952); G. Nalbach, *J. Comp. Physiol. A* **173**, 293 (1993); G. Nalbach and R. Hengstenberg, *ibid.* **174**, 695 (1994); G. Nalbach, *Neuroscience* **61**, 149 (1994).
9. D. C. Sandeman, *J. Comp. Physiol. A* **136**, 361 (1980).
10. M. H. Dickinson, *Soc. Neurosci. Abstr.* **23**, 769 (1997).
11. W. Derham, *Physico-Theology* (W. and J. Innys, London, 1714), chap. 4.
12. R. Galambos, *J. Neurophysiol.* **19**, 424 (1956).
13. J. C. Eccles and C. S. Sherrington, *Proc. R. Soc. London Ser. B* **106**, 326 (1930).
14. S. W. Kuffler and C. Eyzaguirre, *J. Gen. Physiol.* **39**, 155 (1955).
15. To study the minute control muscles in *C. vicina*, we carefully dissected the haltere region from the inside of the thorax, removed the overlaying indirect flight muscles, and stained the preparation for actin with fluorescein isothiocyanate–conjugated phalloidin (Sigma). To construct serial homologies between haltere muscles and wing muscles, we first identified the homologs of the wing axillary sclerites at the base of the haltere. We named the haltere muscles on the basis of their origin and insertion sites according to a nomenclature previously derived for the wing (Table 1).
16. J. A. Miyan and A. W. Ewing, *Philos. Trans. R. Soc. London Ser. B* **311**, 271 (1985); M. H. Dickinson and M. S. Tu, *Comp. Biochem. Physiol. A Physiol.* **116**, 223 (1997).
17. J. W. S. Pringle, *J. Physiol.* **108**, 226 (1949).
18. G. Mickoleit, *Zool. Jahrb. Anat. Ontog. Tiere* **80**, 213 (1962).
19. P. F. Bonhag, *Mem. Cornell Univ. Agric. Exp. Stat.* **285**, 3 (1948).
20. We used low-resistance (2 to 5 Mohms) glass microelectrodes filled with insect saline (*29*) for extracellular recording. The visual stimuli were created on a Tektronix 608 oscilloscope (Tektronix, Beaverton, OR) by a Picasso CRT Image Synthesizer (Innisfree, Cambridge, UK). The stimulus consisted of a square wave grating of light and dark stripes with a spatial frequency of 21° moving at a velocity of 42° s^{-1} to produce a contrast frequency of 2 Hz. The animal was oriented with its longitudinal axis aligned perpendicular to the surface of the CRT screen. The motion stimuli were presented in 16 orientations from 0° to 360° in steps of 22.5°. An orientation of 0° corresponded to upward motion; an orientation of 90° corresponded to lateral motion toward the ipsilateral side. For each fly, the spike frequency was normalized to the maximum response. We recorded from a total of 29 individuals (13 females and 16 males). In 11 animals (6 females and 5 males), we recorded the activities of both B2 and I1 sequentially in the same individual.
21. As with the wing-steering muscles that were studied, haltere muscles B2 and I1 are innervated by a single motoneuron (*33*). Insect synchronous muscles fire one overshooting action potential in response to each spike in their presynaptic motoneuron. It is therefore possible to unambiguously monitor the threshold activity of the motoneurons through the spikes in their target muscles.
22. K. Hausen, *Z. Naturforsch.* **31c**, 629 (1976); R. Hengstenberg, *J. Comp. Physiol.* **149**, 179 (1982).
23. K. Hausen, *Biol. Cybern.* **46**, 67 (1982).
24. The responses of half of the 12 males tested (type I) were indistinguishable from females. The other males tested (type II) showed a bimodal sensitivity, with a second preferred direction shifted 180° relative to the first (Fig. 2, E and G). One possible explanation for the second peak is that it represents the activity of I2. We could not, however, detect any evidence for size or shape classes within spike records from type II males.
25. G. Heide, *Z. Vgl. Physiol.* **59**, 456 (1968).
26. ———, in *BIONA-report 2*, W. Nachtigall, Ed. (Fischer, Stuttgart, Germany, 1983), pp. 35–52.
27. H. Reichert and C. H. F. Rowell, *J. Neurophysiol.* **53**, 1201 (1985); H. Reichert, C. H. F. Rowell, C. Griss, *Nature* **315**, 142 (1985).
28. D. C. Sandeman and H. Markl, *J. Exp. Biol.* **85**, 43 (1980); R. Hengstenberg, D. C. Sandeman, B. Hengstenberg, *Proc. R. Soc. London Ser. B* **227**, 455 (1986); R. Hengstenberg, *J. Comp. Physiol. A* **163**, 151 (1988).
29. A. Fayyazuddin and M. H. Dickinson, *J. Neurosci.* **16**, 5225 (1996).
30. J. R. Trimarchi and R. K. Murphey, *ibid.* **17**, 4700 (1997).
31. R. A. McCrea, in *Behavior Contingent Processing of Vestibular Sensory Signals in the Vestibular Nuclei*, S. M. Highstein, B. Cohen, J. A. Buettner-Ennever, Eds. (New York Academy of Sciences, New York, 1996), pp. 292–303.
32. H. Wolf, *J. Exp. Biol.* **182**, 229 (1993).
33. W. P. Chan, F. Prete, M. H. Dickinson, data not shown.
34. G. Heide, *Zool. Jahrb. Physiol.* **76**, 87 (1971).

35. Supported by grants from NSF (IBN-9723424) and the David and Lucile Packard Foundation to M.H.D.

16 December 1997; accepted 10 February 1998

A Marine Natural Product Inhibitor of Kinesin Motors

Roman Sakowicz, Michael S. Berdelis, Krishanu Ray, Christine L. Blackburn, Cordula Hopmann, D. John Faulkner, Lawrence S. B. Goldstein*

Members of the kinesin superfamily of motor proteins are essential for mitotic and meiotic spindle organization, chromosome segregation, organelle and vesicle transport, and many other processes that require microtubule-based transport. A compound, adociasulfate-2, was isolated from a marine sponge, *Haliclona* (also known as *Adocia*) species, that inhibited kinesin activity by targeting its motor domain and mimicking the activity of the microtubule. Thus, the kinesin-microtubule interaction site could be a useful target for small molecule modulators, and adociasulfate-2 should serve as an archetype for specific inhibitors of kinesin functions.

Eukaryotic cells depend on dynamic microtubule (MT)-mediated events executed by members of the kinesin superfamily. Various kinesins are necessary for cell division (*1*) and for vesicle (*2*) and organelle (*3*) transport. More than 100 kinesin superfamily members are currently known. Different kinesins share a common 350–amino acid motor domain, which is necessary and sufficient for adenosine triphosphate (ATP)–dependent force generation (*4*), attached to a variety of cargo-binding or effector tail domains. The atomic structure of the motor domain (*5–8*) and the basic elements of the kinetic cycle (*9*) are now known. However,

R. Sakowicz, M. S. Berdelis, K. Ray, L. S. B. Goldstein, Department of Pharmacology, Division of Cellular and Molecular Medicine, Howard Hughes Medical Institute, University of California, San Diego, 9500 Gilman Drive, La Jolla, CA 92093–0683, USA.
C. L. Blackburn, C. Hopmann, D. J. Faulkner, Scripps Institution of Oceanography, University of California, San Diego, La Jolla, CA 92093–0212, USA.

*To whom correspondence should be addressed. E-mail: lgoldstein@ucsd.edu

many key elements are still missing from our understanding of kinesin mechanisms. In particular, how changes in the nucleotide binding state modulate kinesin affinity for the MT and how these changes couple to stepping are poorly understood (*10*).

Identification of specific kinesin inhibitors would substantially aid understanding, because such inhibitors could selectively abolish activity in vivo and knowledge about their mechanism of inhibition would allow better insight into enzyme mechanisms. However, no good inhibitors of kinesin motors are currently available except for nucleotide analogs, which are not very useful in vivo because of their lack of specificity.

We looked for kinesin inhibitors in marine sponges, which are a rich source of chemically unique, biologically active compounds (*11*). Marine sponge extracts were tested for disruption of an MT gliding motility assay (*12*). This method allowed an immediate distinction to be made between effects on motility and effects on MT stability. Active extracts were then tested for inhibition of the MT-stimulated kinesin ATPase (*13*). The most promising extract, from the sponge *Haliclona* (also known as *Adocia*) sp., disrupted MT attachment to the kinesin-coated surface in the motility assay and completely inhibited the MT-stimulated kinesin ATPase.

We identified the active compound in the extract and named it adociasulfate-2 (AS-2) (Fig. 1A). AS-2 inhibited the MT-stimulated kinesin ATPase with median inhibitory concentration (IC_{50}) in the low micromolar range (Fig. 1B). The AS-2 structure does not resemble that of nucleotide triphosphates, which suggests a different mode of action from that of known kinesin inhibitors and increases the chances of a narrower activity spectrum. To investigate specificity, we tested AS-2 on various ATPases. Of those tested, the only enzymes substantially inhibited by AS-2 were kinesin superfamily members (Table 1). In addition, we observed no effect of AS-2 on MT polymerization (*14*).

The behavior in the motility assay suggested that AS-2 may interfere with MT binding to kinesin. We tested this hypothesis by performing a kinesin-MT (*15*) cosedimentation assay in the presence of a nonhydrolyzable ATP analog, AMP-PNP, with or without AS-2 (Fig. 2A). Under these conditions, 35 μM AS-2 abolished kinesin binding to MTs. Consideration of the kinesin mechanochemical cycle suggested that the effect on MT binding could be induced by (i) locking kinesin in a weakly binding state resembling the kinesin–adenosine diphosphate (ADP) intermediate through AS-2 binding in the nucleotide pocket or (ii) by direct interference with

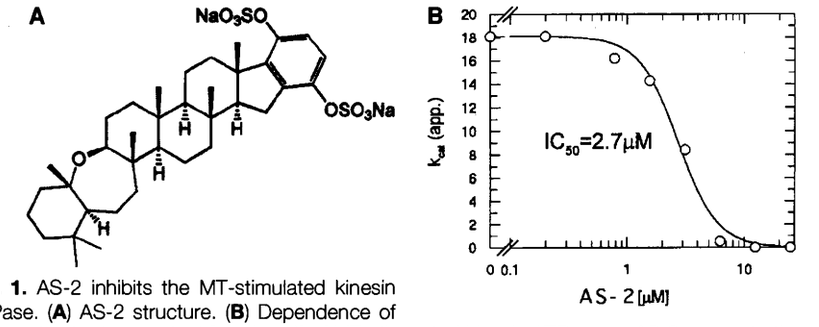

Fig. 1. AS-2 inhibits the MT-stimulated kinesin ATPase. (**A**) AS-2 structure. (**B**) Dependence of apparent catalytic constant [k_{cat} (app.)] of MT-stimulated kinesin ATPase on AS-2 concentration.

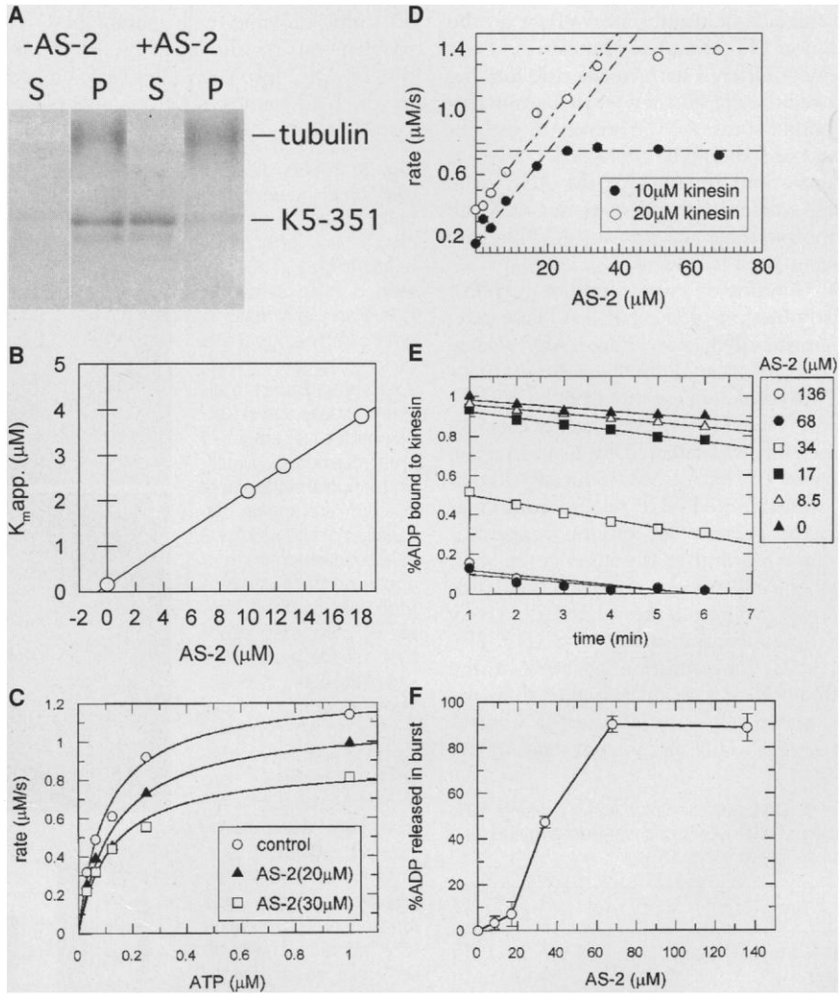

Fig. 2. Biochemical characterization of AS-2 action. (**A**) AS-2 prevents kinesin binding to microtubules. The monomeric kinesin protein K5–351 (3.5 μM) was preincubated with MT (3.6 μM), MgAMP-PNP (2 mM), and with (+AS-2) or without (–AS-2) 35 μM AS-2. After 10 min, the mixture was centrifuged at 80,000*g* for 30 min, and supernatants (S) and pellets (P) were analyzed by SDS–polyacrylamide gel electrophoresis. (**B** and **C**) AS-2 inhibition is competitive with MT but not with ATP. Initial rate measurements were done at room temperature with the use of a malachite green assay (*13*). ATP concentration dependence was determined by a coupled enzymatic assay with pyruvate kinase and lactate dehydrogenase, monitoring changes in absorbance at 340 nm. (*21*) (B) Apparent K_m for MTs depends linearly on AS-2 concentration. The intercept with the *x* axis gives an estimated K_i value of 0.8 μM. (C) Apparent K_m for ATP does not depend on AS-2 concentration; only V_{max} is affected. (**D**) AS-2 stimulates the basal kinesin ATPase without MTs. (**E** and **F**) AS-2 induces a burst of ADP release (*22*). (E) An example of the experimental trace. (F) The magnitude of the burst of ADP release depends on AS-2 concentration.

the MT-binding site. Steady-state kinetic measurements demonstrated that AS-2 inhibition was competitive with MTs and could be totally reversed by high MT concentrations. The apparent Michaelis constant (K_m) for MT depended linearly on AS-2 concentration (Fig. 2B) [inhibition constant (K_i) = ~0.8 μM]. In contrast, varying the ATP concentration did not affect the overall shape of the kinetic curves. Maximum reaction velocity (V_{max}) was progressively lower at higher AS-2 concentrations (Fig. 2C), demonstrating that excess ATP could not outcompete AS-2 inhibition. Additional evidence against AS-2 binding at the nucleotide pocket comes from the lack of an inhibitory effect on the basal, non-MT–stimulated kinesin ATPase. If AS-2 interfered with nucleotide binding or locked the enzyme in a particular nucleotide-bound state, ATP turnover in the absence of MT should be decreased. However, concentrations up to 136 μM AS-2 (the highest concentration tested) not only did not inhibit the basal kinesin ATPase rate but stimulated it instead.

MT binding to kinesin induces ~1000-fold stimulation of the basal ATPase rate, owing primarily to accelerated ADP release (*16*). In the absence of MTs, AS-2 stimulated the basal ATPase rate from ~0.01/s to ~0.06/s (Fig. 2D). To test whether this rate acceleration was affected by a mechanism analogous to that of MT-induced stimulation, we examined ADP release from kinesin in the presence of varying concentrations of AS-2 and in the absence of MTs. Bursts of ADP release were observed (Fig. 2E); their magnitude correlated positively with the concentration of AS-2 (Fig. 2F). The AS-2 concentration at 50% of the maximum burst was much higher than the K_i estimated from steady-state MT competition assays. This discrepancy may reflect different affinities for AS-2 by different nucleotide states of kinesin. Steady-state kinetic measurements of K_i reflect the affinity of the most tightly bound state of the cycle, which includes several intermediates (kinesin-ATP, kinesin–ADP–inorganic phosphate, kinesin-ADP, and so on). In contrast, the ADP release experiment involved only one state, kinesin-ADP, which has the lowest affinity for the MT (*17*).

We also investigated the in vivo effects of AS-2. Preliminary experiments demonstrated that AS-2 had no effect on HeLa cell proliferation. However, AS-2 is a fairly large molecule (molecular weight 738) with two charged sulfate moieties and may have difficulty crossing cell membranes. This problem can be alleviated by direct injection of AS-2 into early *Drosophila* embryos, in which 13 rounds of mitosis take place in a syncytium. The first seven divisions are synchronized and occur at the center of the egg. During the next three divisions, most nuclei move to the egg surface and then divide three times in partially open cell buds (*18*). Thus, drugs injected into these early embryos will have access to many mitotic nuclei at the egg surface during the last three divisions. We injected three different AS-2 concentrations (1300 μM, 130 μM, and 65 μM) (*19*); 130 μM AS-2 arrested all nuclear divisions immediately at the point of injection (Fig. 3B); 65 μM AS-2 caused less severe phenotypes with more distinct abnormalities. At the injection site, we found spindles and MT asters without chromosomes (Fig. 3, D and F), mats of unattached MTs (Fig. 3D), and chromosomes apparently detached from the spindle (Fig. 3F). These effects could be

Table 1. Concentrations of AS-2 causing 50% inhibition of ATPase. Rates were determined by a malachite green assay (*13*).

Enzyme	IC_{50}
Rabbit kidney ATPase*	>136 μM†
Apyrase	>136 μM†
Myosin II (EDTA)‡	75 μM
CENP-E§	10 μM#
K5-351‖	2 μM**
K411¶	2 μM**
T1-γ††	2 μM**
Pyruvate kinase	>136 μM†

*Obtained from Sigma (A2414). †Enzyme was not inhibited by 50% at the highest used inhibitor concentration of 136 μM. ‡EDTA activated ATPase. §Construct containing 473 amino acids of *Xenopus* CENP-E. ‖Construct containing amino acids 5 through 351 of *Drosophila* kinesin. ¶Construct containing amino acids 1 through 411 of *Drosophila* kinesin. #At 6 μM tubulin. **At 2 μM tubulin. ††Construct containing 778 amino acids of *T. lanuginosus* kinesin-like protein.

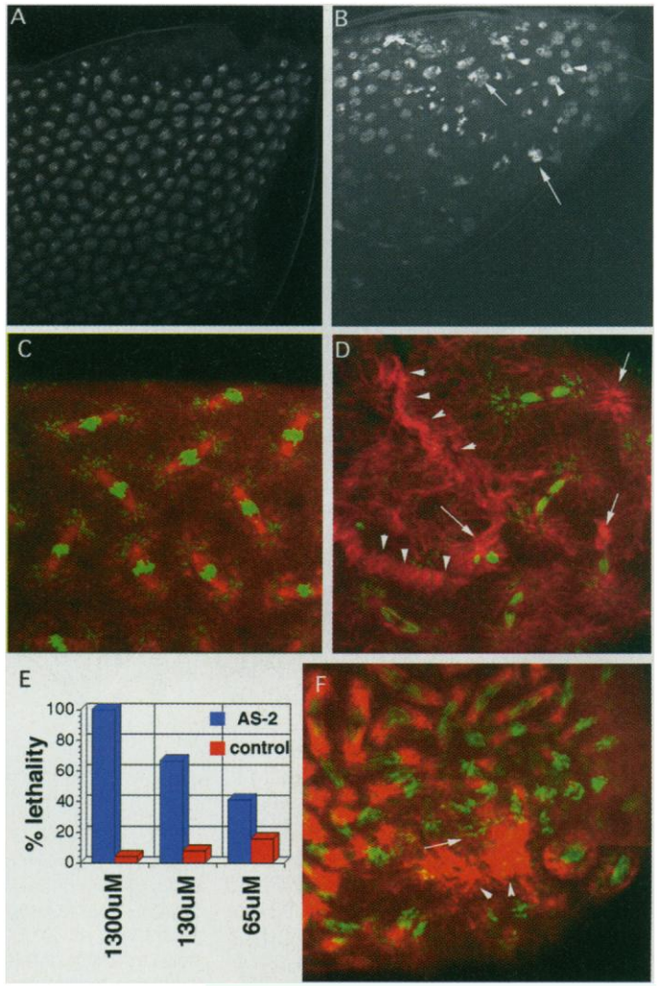

Fig. 3. Effects of AS-2 injection in the early precellular blastoderm embryo of *Drosophila melanogaster* (*23*). In double-stained images, tubulin is red and chromatin is green. (**A**) The nuclei of a buffer-injected control embryo continued to divide normally and develop until the late stages of embryogenesis; interphase nuclei at the site of injection are shown. (**B**) Injection of 130 μM AS-2 halted development and appeared to cause apoptotic cell death. A variety of chromatin structure defects around the site of injection, from extremely compact nuclei (arrows) to big, complex, semi-compact chromatin aggregates are shown. Some nuclei (arrowheads) were clearly pycnotic. (**C**) In an embryo injected with buffer, spindle formation and chromosome separation took place normally; an early precellular blastoderm embryo where all the nuclei were at mid-metaphase is shown. (**D**) Striking defects in MT and chromosome organization were seen in embryos injected with 65 μM AS-2. Many extra MT asters (arrows) not attached to chromatin were near the site of injection. Large knots of microtubules (arrowheads) were also visible without associated chromatin. (**E**) Percentage of *Drosophila* embryos dying after the injection of various AS-2 concentrations. Controls were injected with buffer only. Each data point summarizes results for 50 injected embryos. (**F**) In embryos injected with AS-2, some chromosomes were apparently detached from the spindles (arrows). We also observed large knots of MTs (arrowheads) that were devoid of chromatin. In (C), (D), and (F), tubulin is red and chromatin is green.

accounted for by loss of function of various kinesin superfamily members (*20*). Control embryos injected with buffer alone did not exhibit any of these phenotypes (Fig. 3, A and C); the majority of them survived until the gastrula stage (Fig. 3E), when they were fixed and stained. Embryos injected in the post-cellularization stage developed normally, confirming that AS-2 was unable to cross cell membranes.

Our results demonstrate that AS-2 specifically inhibits kinesin activity by interfering with MT binding. This mechanism is unlike that of any known kinesin (or other motor) inhibitor and may be generated by AS-2 emulating tubulin binding to a portion of the MT-binding site of kinesin. AS-2 is also a potent toxin, which when delivered intracellularly may ablate several, if not all, aspects of kinesin-superfamily–mediated transport. AS-2 and its derivatives have many potential applications. When made membrane permeant, AS-2 and its derivatives would be likely to be efficient antimitotic or antitransport drugs for studying kinesin functions or might be therapeutic agents. The existence of a kinesin atomic structure may allow the rational design of molecules based on AS-2 and the development of specific inhibitors for kinesin families and subfamilies, thus leading to precise chemical intervention. Finally, the ability of AS-2 and its derivatives to mimic the activity of the MT may allow modification of surfaces or other substrates with AS-2 to create artificial kinesin tracks.

REFERENCES AND NOTES

1. A. S. Kashina, G. C. Rogers, J. M. Scholey, *Biochim. Biophys. Acta* **1357**, 257 (1997); C. E. Walczak and T. J. Mitchison, *Cell* **85**, 943 (1996).
2. M. P. Sheetz, *Cell Struct. Funct.* **21**, 369 (1996).
3. N. Hirokawa, *ibid.*, p. 357.
4. R. J. Stewart, J. P. Thaler, L. S. B. Goldstein, *Proc. Natl. Acad. Sci. U.S.A.* **90**, 5209 (1993).
5. F. J. Kull, E. P. Sablin, R. Lau, R. J. Fletterick, *Nature* **380**, 550 (1996).
6. E. P. Sablin, F. J. Kull, R. Cooke, R. D. Vale, R. J. Fletterick, *ibid.*, p. 555.
7. G. Woehlke *et al.*, *Cell* **90**, 207 (1997).
8. H. Sosa *et al.*, *ibid.*, p. 217.
9. D. D. Hackney, *Annu. Rev. Physiol.* **58**, 731 (1996).
10. J. Howard, *ibid.*, p. 703.
11. D. J. Faulkner, *Nat. Prod. Rep.* **14**, 259 (1997) and references therein.
12. Tl-γ (a kinesin superfamily member from the fungus *Thermomyces lanuginosus*) was adsorbed to a glass cover slip and supplemented with MTs, 2 mM Mg-ATP, and sponge extracts in dimethyl sulfoxide (5% final concentration) in 80 mM Pipes (pH 6.8), 1 mM $MgCl_2$, and 1 mM EGTA. Motility was scored by standard methods (*4*).
13. T. P. Geladopoulos, T. G. Sotiroudis, A. E. Evangelopoulos, *Anal. Biochem.* **192**, 112 (1991).
14. The effect of AS-2 on MT polymerization was tested by a pelleting assay with tubulin polymerized at 36°C (with 1 mM guanosine triphosphate and without paclitaxel) and increasing AS concentrations up to 130 μM.
15. Subsequent binding and kinetic measurements were performed on a bacterially expressed *Drosophila* kinesin heavy-chain fragment (K5–351) containing amino acids 5 through 351 and a hexahistidine tag at the COOH-terminus. Soluble protein was purified from isopropyl-β-D-thiogalactopyranoside–induced bacterial cells by a single round of affinity chromatography on Ni-NTA-agarose (Qiagen), concentrated by microfiltration, and frozen in aliquots in liquid nitrogen.
16. D. D. Hackney, *Proc. Natl. Acad. Sci. U.S.A.* **85**, 6314 (1988).
17. L. Romberg and R. R. Vale, *Nature* **361**, 168 (1993).
18. J. A. Campos-Ortega and V. Hartenstein, *The Embryonic Development of* Drosophila melanogaster (Springer-Verlag, Berlin, 1985).
19. The concentrations reported refer to the solution in the injection apparatus. During injection, only a small amount of liquid was delivered to the embryo. The exact value could not be measured but was estimated as less than 2% of the embryonic volume [for example, see J. Minden, *BioTechniques* **20**, 122 (1996)]. Therefore, the actual in situ concentration of AS-2 was about 50 times lower than the needle concentration.
20. N. R. Barton and L. S. Goldstein, *Proc. Natl. Acad. Sci. U.S.A.* **93**, 1735 (1996).
21. T. G. Huang and D. D. Hackney, *J. Biol. Chem.* **269**, 16493 (1994).
22. D. D. Hackney's method [*ibid.*, p. 16508] was modified as follows: 80 μM kinesin was preincubated with [α-^{32}P]ATP at room temperature for 15 min and stored on ice. One-microliter aliquots were diluted into 100 μl of "chase mix" containing pyruvate kinase (0.5 mg/ml), 2 mM phosphoenolpyruvate, and AS-2. At different times, 5-μl aliquots of the chase mix were quenched in 100 μl of 1 M Hcl, 1 mM ATP, and 1 mM ADP. The amount of ADP accessible to pyruvate kinase and converted to ATP was determined by thin-layer chromatography on PEI-cellulose and phosphoImager (Molecular Dynamics) quantitation.
23. Embryos were collected every 20 min and dechorionated. They were desiccated for 7 min and pressure-injected with either the AS-2 solution in injection buffer [5 mM KCl and 100 mM sodium phosphate (pH 7.5)] or with buffer alone as a control. Batches of 20 embryos were injected, and at least three batches were injected for each concentration of AS-2 and the control. After injection, the embryos were developed for 20 to 30 min at room temperature inside a moist chamber and were fixed, devitelinized, immunostained for tubulin (Fig. 3, C, D, and F), and counterstained with 4′,6′-diamidino-2-phenylindole (DAPI) (0.01 mg/ml) (Fig. 3, A through D and F). Images were recorded on a Bio-Rad MRC-1024 confocal laser scanning microscope using LaserSharp software.

24. We thank the Republic of Palau and the State of Koror for marine research permits, M. K. Harper for identification of the sponge, E. Komives and B. Yang for advice on enzyme kinetics, S. Farlow for kinesin constructs, and K. Wood for *Xenopus* CENP-E constructs. This work was supported by the Cancer Research Fund of the Damon Runyon–Walter Winchell Foundation Fellowship (R.S.), by NIH (L.S.B.G., C.L.B., and D.J.F.), and by the California Sea Grant College Program (C.L.B., C.H., and D.J.F.). L.S.B.G. is an investigator at the Howard Hughes Medical Institute.

29 December 1997; accepted 13 February 1998

The Involvement of Cell-to-Cell Signals in the Development of a Bacterial Biofilm

David G. Davies, Matthew R. Parsek, James P. Pearson, Barbara H. Iglewski, J. W. Costerton, E. P. Greenberg*

Bacteria in nature often exist as sessile communities called biofilms. These communities develop structures that are morphologically and physiologically differentiated from free-living bacteria. A cell-to-cell signal is involved in the development of *Pseudomonas aeruginosa* biofilms. A specific signaling mutant, a *lasI* mutant, forms flat, undifferentiated biofilms that unlike wild-type biofilms are sensitive to the biocide sodium dodecyl sulfate. Mutant biofilms appeared normal when grown in the presence of a synthetic signal molecule. The involvement of an intercellular signal molecule in the development of *P. aeruginosa* biofilms suggests possible targets to control biofilm growth on catheters, in cystic fibrosis, and in other environments where *P. aeruginosa* biofilms are a persistent problem.

Certain bacteria, such as the fruiting bacteria, communicate with each other to form structured macroscopic groups (*1*, *2*). Recently, it has become apparent that in appropriate environments, common bacteria exhibit similar social behavior. Microscope observations of living bacterial biofilms attached to a glass surface have revealed that these sessile microbial biofilm populations have a complicated structural architecture (*3*, *4*). Biofilms of mixed bacterial communities and of individual species such as *Pseudomonas aeruginosa* that develop on solid surfaces exposed to a continuous flow of nutrients form thick layers consisting of differentiated mushroom- and pillar-like structures separated by water-filled spaces. The structures consist primarily of an extracellular polysaccharide (EPS) matrix or glycocalyx in which the bacterial cells are embedded (*5*). The finding that *P. aeruginosa* produces at least two extracellular signals involved in cell-to-cell communication and cell density-dependent expression of many secreted virulence factors suggests

D. G. Davies and J. W. Costerton, Center for Biofilm Engineering, Montana State University, Bozeman, MT 59717–3980, USA.
M. R. Parsek and E. P. Greenberg, Department of Microbiology, University of Iowa, Iowa City, IA 52242, USA.
J. P. Pearson and B. H. Iglewski, Department of Microbiology and Immunology, University of Rochester, Rochester, NY 14642, USA.

*To whom correspondence should be addressed. E-mail: epgreen@blue.weeg.uiowa.edu